DOI: 10.1002/stco.202200047

Balázs Kövesdi, László Dunai

ARTICLE

Patch loading resistance of slender plate girders with multiple longitudinal stiffeners

There is currently no reliable and simple design method available in international literature for the determination of the patch loading resistance of slender plate girders having multiple longitudinal stiffeners. The current research focuses on the patch loading resistance of girders having multiple longitudinal stiffeners. An advanced numerical model is developed and verified by own laboratory test results. A numerical parametric study is executed to investigate the load-carrying capacity of girders having typical bridge geometries. Analysing the numerical simulation results, the structural behaviour obtained is classified based on the stiffener stiffness. Effect of the different geometrical parameters on the patch loading resistance is evaluated with special focus on the stiffener stiffness and distance between the longitudinal stiffeners. The failure modes depending on stiffener stiffness are investigated and the local buckling type failure is characterised by minimum stiffness. For this specific failure mode, an improved design method is developed, giving reliable resistance within the analysed parameter range. The presented resistance model is consistent with the design philosophy of EN 1993-1-5. The applicability of the improved design equation has been investigated for multiple stiffener places in unequal distances, which is the common case in praxis, and for bending and transverse force (M–F) interaction.

Keywords patch loading; stiffened girders; bending and shear interaction

1 Introduction

In the case of slender plate girders with longitudinal stiffeners, it is known that the patch loading resistance model of EN 1993-1-5 [1] had a large scatter and it can lead to significant underestimation of the resistance. Numerous previous experimental and numerical research programmes [2–10] have studied the patch loading resistance of longitudinally stiffened girders to develop a reliable resistance model. After all, there is currently no reliable and simple design method available in international literature. The main part of the previous investigations focuses on the patch loading resistance of girders having one longitudinal stiffener. In the bridge design, however, usually not only one stiffener is applied on the web but multiple stiffeners distributed quasiuniformly along the plate width. For these cases, the applicability of the previously developed design methods is not proved. It is also known that the design method of EN 1993-1-5 [1] does not consider the location of longitudinal stiffeners properly, even having one stiffener placed on the web. Therefore, the focus of the current article is on the investigation of the patch loading resistance of slender web girders with multiple longitudinal stiffeners. In the current bridge design praxis, launching (Fig. 1a) is one of the mostly used erection methods for steel bridges due to its numerous advantages.

It might introduce a large local concentrated force within the web which might cause web crippling-type failure. In many cases to avoid this failure mode, additional vertical stiffeners are welded on the slender web, as shown in Fig. 1b. However, this solution is usually extremely cost and time-consuming. Numerical simulation results for existing bridge girders show in many cases that these stiffeners can be eliminated by applying a more appropriate design method for the patch loading resistance calculation for longitudinally stiffened girders. The research aim of the current study is a comprehensive investigation of the web-crippling phenomena of longitudinally stiffened girders with multiple stiffeners and improvement of EN 1993-1-5 [1]-based patch loading resistance model.

Within the research programme, all the existing experimental, analytical, and numerical investigations were overviewed, evaluated, and compared. A laboratory test programme is designed and executed to investigate the patch loading resistance of girders with multiple longitudinal stiffeners. The test results showed the dominant

a)

b)

Fig. 1 Typical layout of the launched box section bridge a) launching phase and b) internal stiffeners to avoid patch loading failure

failure modes and the efficiency of the longitudinal stiffeners. Based on the test results, a numerical model is developed and validated to accurately determine the patch loading resistance of girders with multiple longitudinal stiffeners. A numerical parametric study is executed to investigate the load-carrying capacity of girders having typical bridge geometries. Based on a large number of numerical simulations, the structural behaviour is studied and the obtained failure modes are classified based on the stiffness of the stiffener. The effect of each geometrical parameter on the patch loading resistance is evaluated with special focus on the stiffness of the stiffener and distance between the longitudinal stiffeners. Finally, an improved design method is developed for girders with multiple stiffeners. The applicability of the developed design method has been also checked for girders having multiple stiffeners placed in unequal distances, which is a common situation in case of existing bridges. The applicability of the previously developed M–F interaction equation has been also studied by applying the new patch loading resistance model. The M–F interaction check is a crucial point for bridge launching; therefore, the accuracy of the new resistance model regarding the M–F interaction check has large importance. The research work is completed according to the following research strategies:

- literature review in the topic of the previous investigations on the patch loading resistance;
- conducting laboratory tests on eight large-scale test specimens to determine the patch loading resistance and analysing the dominant failure modes;
- development and validation of an advanced numerical model based on shell elements with variable geometry and different longitudinal stiffener configurations;
- a numerical parametric study to investigate the observed failure modes and the effect of the different geometric parameters on the patch loading resistance;
- a design method development for girders with longitudinal stiffeners;
- a numerical parametric study using unequal stiffener distances to check the application range of the improved design method; and
- a numerical parametric study to check the M–F interaction behaviour to prove the applicability of the new patch loading resistance model.

2 Literature review: Previous research results

In international literature, a large number of previous investigations can be found dealing with the determination of patch loading resistance. The main parts of these investigations focus on the experimental and numerical investigation of the web crippling-type failure and try to develop a more accurate analytical design equation. Within these improved design methods, the effect of longitudinal stiffener is usually implemented in the critical load (F_{cr}) by improving the buckling coefficient (k_F). The reduction factor (χ_F), however, is usually determined by the same equation for stiffened and unstiffened girders. The design method of EN 1993-1-5:2006 [1] for the patch loading resistance calculation uses the analytical mechanical model of Lagerqvist and applies reduction factor developed by Graciano, Lagerqvist and Johannson [2–6]. In recent years, the patch loading resistance model has been widely investigated and the reduction factor has been statistically evaluated. Based on the extensive research work of Davaine [7], Gozzi [8] and Chacón et al. [9], the patch loading resistance model has been improved and the calculation method of the effective loading length has been enhanced. Based on the statistical evaluation of Mirambell et al. [10], a new reduction factor calculation method has been also implemented into the second generation of Eurocodes, in EN 1993-1-5 [11]. According to this improved design model, the resistance can be calculated by Eq. (1) in case of patch loading 'type a' according to EN 1993-1-5 Fig. 6.1, and this case is investigated in the current article.

$$F_{Rd} = \chi_F \cdot \frac{l_y \cdot f_{yw} \cdot t_w}{\gamma_{M1}} \leq 1.0 \tag{1}$$

The reduction factor due to local buckling χ_F may be obtained by Eqs. (2) to (5).

$$\chi_F = \frac{1.0}{\phi_F + \sqrt{\phi_F^2 - \bar{\lambda}_F}} \leq 1.0 \tag{2}$$

where

$$\phi_F = \frac{1}{2}\left(1 + \alpha_{F0} \cdot \left(\bar{\lambda}_F - \bar{\lambda}_{F0}\right) + \bar{\lambda}_F\right) \tag{3}$$

$$\bar{\lambda}_F = \sqrt{\frac{l_y \cdot t_w \cdot f_{yw}}{F_{cr}}} \tag{4}$$

$$\alpha_{F0} = 0.75\ \alpha_{F0} = 0.75\ \ \bar{\lambda}_{F0} = 0.50 \quad \text{if } \gamma_{M1} = 1.10\ \gamma_{M1} = 1.10 \tag{5}$$

(calibrated to the given α_{F0} and λ_{F0} values).

The effective loaded length (l_y) is given by Eq. (6).

$$l_y = s_s + 2 \cdot t_f \cdot \left(1 + \sqrt{\frac{b_f}{t_w}}\right) \tag{6}$$

The critical load (F_{cr}) may be calculated by Eq. (7) using the buckling coefficient according to Eqs. (8) to (9) for longitudinally stiffened girders.

$$F_{cr} = 0.9 \cdot k_F \cdot E \cdot \frac{t_w^{\ 3}}{h_w} \tag{7}$$

$$k_F = 6 + 2 \cdot \left(\frac{h_w}{a}\right)^2 + \left(5.44 \cdot \frac{b_1}{a} - 0.21\right) \cdot \sqrt{\gamma_s} \tag{8}$$

$$\gamma_s = 10.9 \cdot \frac{I_{sl}}{h_w \cdot t_w} \leq 13 \cdot \left(\frac{a}{h_w}\right)^3 + 210 \cdot \left(0.3 - \frac{b_1}{a}\right) \tag{9}$$

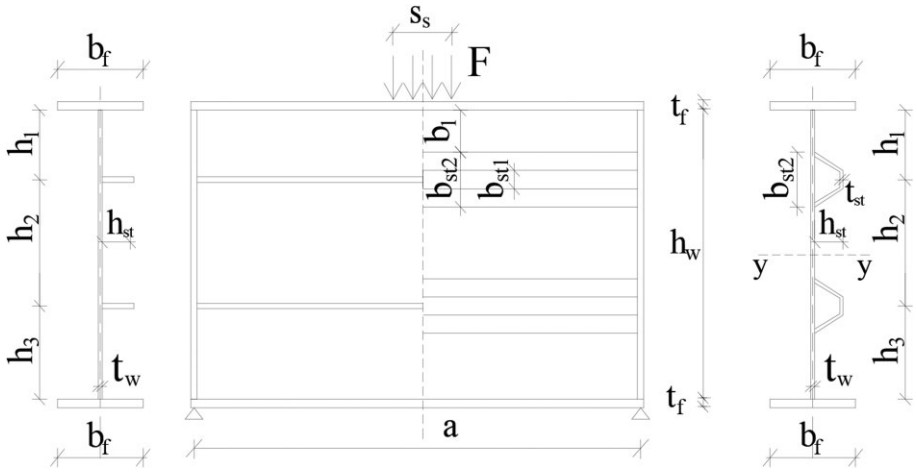

Fig. 2 Used geometry and investigated structural layouts with open and closed section stiffeners

The used notations and the layout of the analysed girder geometries are shown in Fig. 2.

It is well known that the Eurocode-based design method is reliable and gives accurate patch loading resistance for unstiffened girders. However, it does not lead to accurate and reliable resistance for longitudinally stiffened girders and have relatively large scatter. Therefore, an intensive research programme was completed to improve the patch loading resistance model in the frame of the COMBRI-Project [12]. Within this research work, Seitz [13] conducted laboratory tests and performed a numerical parametric study to determine the patch loading resistance for different girder geometries and stiffener sizes. Based on the extensive numerical study, an improved design method was developed considering the interpolation between plate-like and column-like behaviour of the web. The proposed design method gave accurate results for the analysed girder geometries; however, it is quite complex and difficult to use in the design. Davaine [7] also executed a numerical parametric study to investigate the critical load and the ultimate resistance of longitudinally stiffened girders. Based on her investigations, it was found that the main reason of the difference within the analytical and numerical results comes from the fact that the web crippling-type failure can occur in the upper or in the lower subpanel and the design method does not follow the correct trend for both cases. Therefore, an enhanced design method was developed considering the failure mode of the different subpanels (failure in the upper or lower subpanel). This design equation follows the trend of the numerical simulations and gives much closer resistance to the numerically calculated values. However, this design equation is developed for girders with one stiffener, and it cannot be applied for multiple stiffened girders. Graciano and Lagerqvist also studied in 2003 the critical buckling load related to patch loading for longitudinally stiffened girders [14]. The research was continued by Graciano and Mendes in 2014 [15]. Based on their extensive investigations, the relevant values of the buckling coefficient (k_F) were determined for all investigated girder geometries, and a design equation was developed to determine the buckling coefficient (k_F). However, further studies of Graciano [16] pointed out that the aforementioned design methods should be improved. The best design equation for the patch loading resistance calculation can result in 20 % to 60 % difference (underestimation) compared to the measured or numerically simulated resistances. Therefore, the improvement of the patch loading resistance model is still an important task within the design of longitudinally stiffened girders. Based on the literature review, it can be also concluded that all the previous researchers were mainly focused on stiffened girders having one longitudinally stiffener and no significant investigation can be found on girders having multiple longitudinal stiffeners, which is the topic of the current article. Therefore, the present study is a unique analysis and gives new aspects to the design of box section steel bridges.

3 Experimental investigations

An experimental research programme was conducted at the Budapest University of Technology and Economics, Department of Structural Engineering, between 2015 and 2016. These laboratory tests are used as background for the numerical model verification and validation and gave intention on the stability failure mode characterisation and prove of the expected structural behaviour of the longitudinal stiffeners. Within the laboratory test programme, eight specimens (four different configurations) were investigated, as shown in Fig. 3.

Two girders had no stiffeners (unstiffened: reference specimens) and six specimens had two or three longitudinal stiffeners placed on the web. For each specimen, the longitudinal stiffeners were uniformly distributed along the girder depth. The geometry of the specimens is shown in Fig. 3, and the measured load displacement curves are presented in Fig. 4.

All specimens were manufactured with a web plate of 500×4 mm and flange plates of 150×10 mm. The length of the specimens was constant, 1050 mm. The stiffener size and numbers were varied within the test programme. Two stiffener sizes are applied, 40×4 mm and 60×4 mm

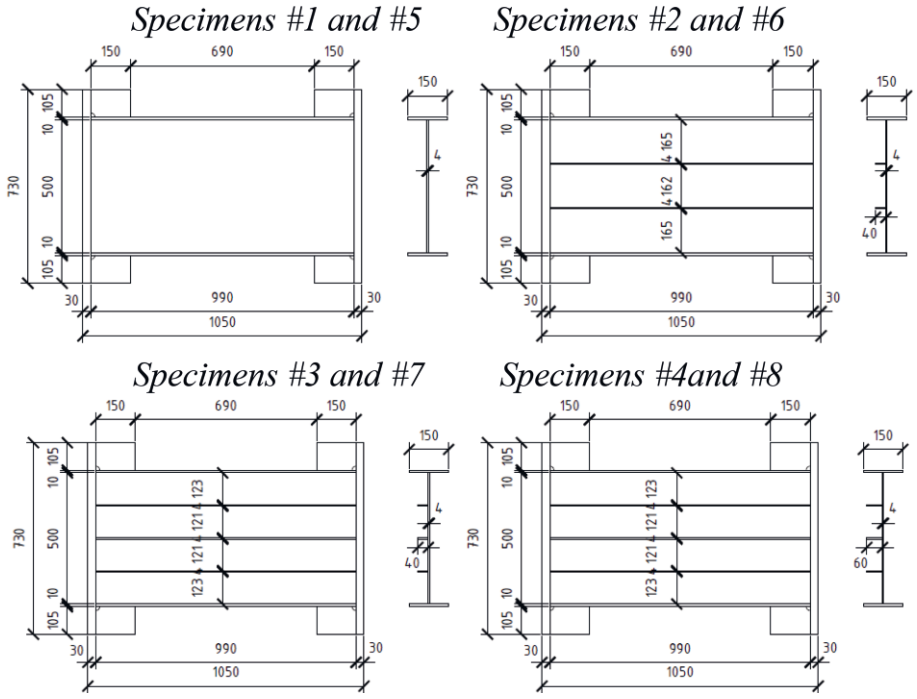

Fig. 3 Geometry of the test specimens

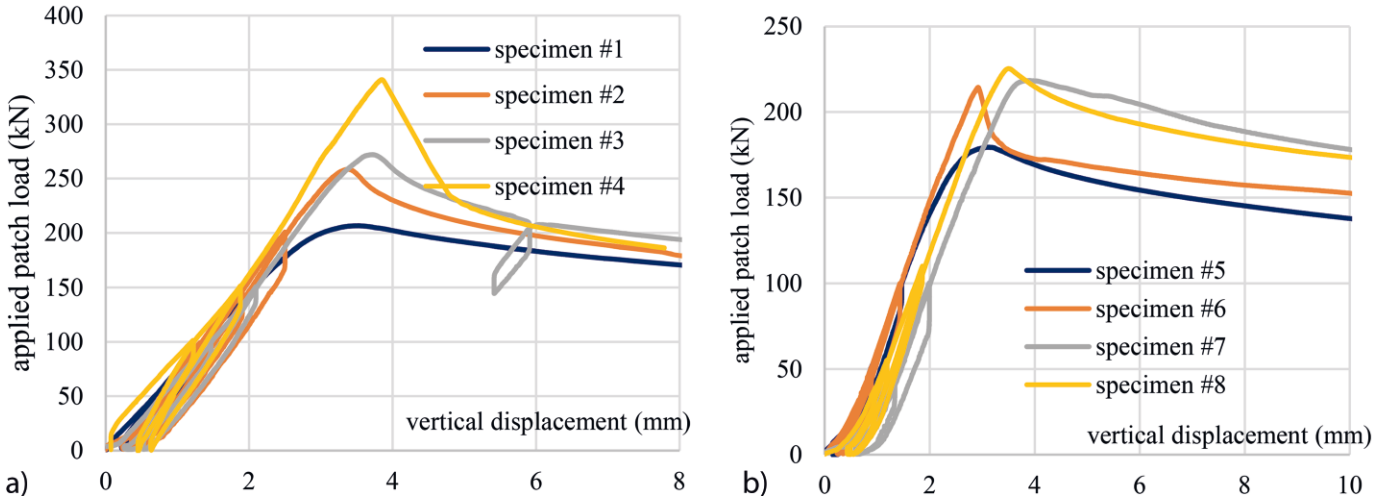

Fig. 4 Load–displacement curve of specimens #1 to 8

Tab. 1 Test specimens and patch loading resistances

Specimen	Stiffener number	Stiffener size	γ_s	s_s [mm]	f_{yw} [MPa]	f_{uw} [MPa]	$F_{R,test}$ [kN]	$F_{R,test,mod}$ [kN]	$F_{R,num}$ [kN]	Difference [%]
#1	0	–	0	200	286	392	206.4	224.6	204.6	–0.87
#2	2	40–4	27.3	200	318	405	258.4	252.9	254.8	–1.39
#3	3	40–4	27.3	200	311	400	270.9	271.2	266.8	–1.54
#4	3	60–4	80.6	200	314	405	320.4	317.6	268.2	–16.29
#5	0	-	0	100	308	392	180.2	182.1	176.5	–2.05
#6	2	40–4	27.3	100	343	444	214.3	194.5	207.9	–3.45
#7	3	40–4	27.3	100	299	394	218.4	227.4	191.6	–12.27
#8	3	60–4	80.6	100	311	393	223.8	223.9	208.9	–6.66
Average					311.3	403.1				–5.6
CoV										1.04

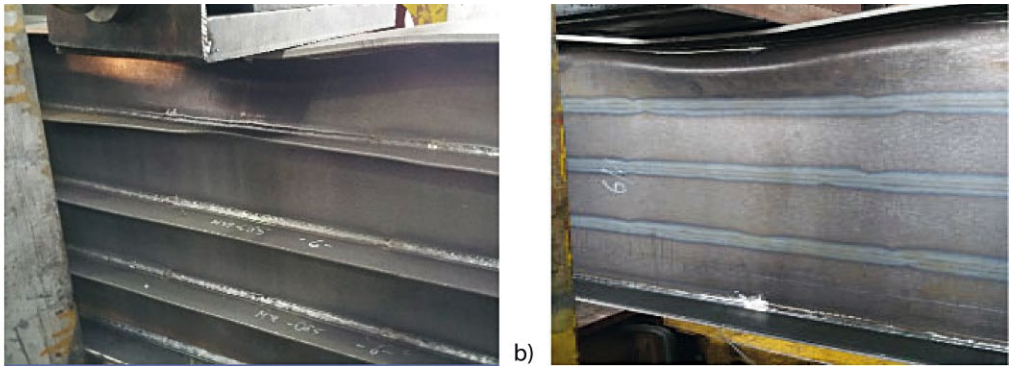

Fig. 5 The typical obtained failure mode of the test specimens

flat plate stiffeners. Specimens #1 to 4 are loaded with loading length of s_s = 200 mm; specimens #5 to 8 are loaded with s_s = 100 mm. Tab. 1 summarises the applied stiffener number and sizes and also gives the measured resistances ($F_{R,test}$). The material properties of the different web plates had differences; therefore, the measured resistances are adjusted based on the material test results to make them comparable. The adjusted resistances noted by $F_{R,test,mod}$ together with the yield and ultimate strength of the web plate are also given in Tab. 1. For the calculation of the adjusted resistance, the ratio of the average and actual yield strength of the web (given in Tab. 1) have been used as conversion factors. The adjusted resistances show the differences coming from the structural layout and/or imperfections of the specimens.

The typical failure mode of the test specimens is shown in Fig. 5, which is always the local web crippling of the subpanels between the loaded flange and the upper longitudinal stiffener. The test programme has been separately published with all details in [17]. The main conclusions of the test results were that relatively small stiffeners are strong enough to localise the failure mode within the web subpanel and eliminate global buckling of the entire web. This observation drew our attention on the fact that the separation of the failure modes (local and global) could be efficient, and it could be made based on the relative stiffness of the stiffeners. As the test results proved relatively weak stiffeners can be effective to eliminate global buckling, the further focus of the research programme is put on the local buckling resistance calculation of the web subpanels under patch load.

4 Numerical investigations

4.1 Development of the numerical model

The developed numerical model applied for the patch loading resistance calculation is shown in Fig. 6 for two test specimens. It is a full shell model using four-node thin shell elements. The numerical model is developed in Ansys [18]. The two end plates are pinned, supported along the lower edges and laterally supported to eliminate the rotation of the end cross sections. The transverse load is applied in the middle of the test specimens. To consider the load introduction plate (which had a large stiffness compared to the upper flange), the rotational degrees of freedoms (DOFs) are coupled at the load introduction length at the location of the patch load. All the applied support and load conditions refer to the laboratory test layout.

The numerical model is used for the determination of the critical (F_{cr}) and ultimate load (F_{ult}) of the analysed girders. The critical load is determined using linear buckling analysis (LBA). The ultimate load is determined by geometric and material nonlinear analyses using equivalent geometric imperfections (GMNIA).

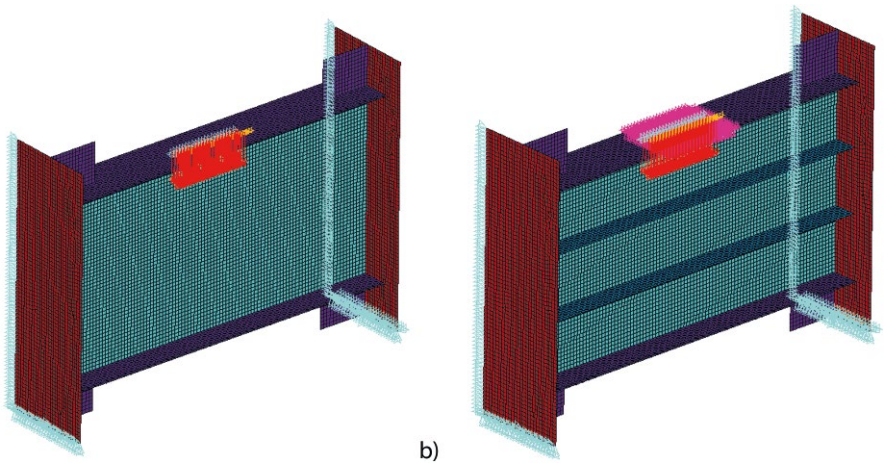

Fig. 6 Numerical model of test specimens

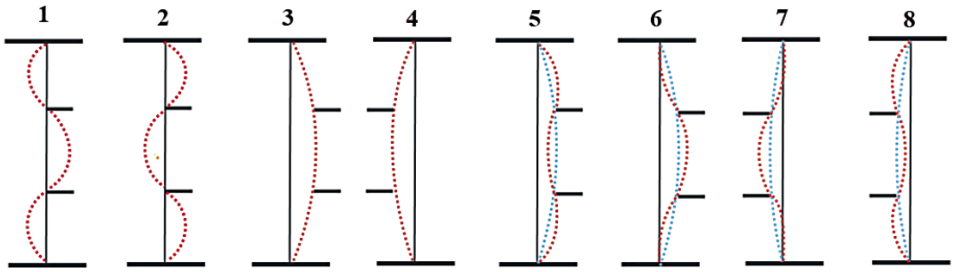

Fig. 7 Analysed imperfection shapes: a combination of local and global imperfections

4.2 Material model and imperfections

Imperfections are highly important for the patch loading resistance calculation as proved by Kövesdi et al. [17]. A detailed imperfection sensitivity analysis is executed before the numerical parametric study. The analysed imperfection shapes for a specimen having two longitudinal stiffeners are presented in Fig. 7. A similar study has been executed for girders having one and three longitudinal stiffeners on the web.

Global and local imperfection shapes are both considered with an amplitude of $h_w/200$ for the global, and $b_i/200$ for the local buckling, where h_w is the entire web depth and b_i is the depth of the web subpanels. The most detrimental imperfection layout is selected for the determination of the patch loading resistance, and it was used in further numerical parametric study. More details on the imperfection sensitivity analysis can be found in [17].

In the presented research programme, two material models are applied, which are similar in model types and characters, but different in its characteristic values. The first one is used to model validation and the second one to numerical parametric study. In both models, linear elastic hardening plastic material model with von Mises yield criterion is used, applying the isotropic hardening rule in the plastic domain. The material is assumed to behave linearly elastic and obey Hooke's law with a Young' modulus equal to 210,000 MPa up to the yield stress. Thereafter and until it reaches the ultimate stress, the material is assumed to behave linearly with a hardening modulus. The ultimate strength is defined by $\varepsilon = 12\,\%$, which fits to the average material tests. Within this material model, the hardening modulus is set between 680 and 1250 MPa depending on the analysed specimen.

4.3 Model verification and validation

At first, the numerical model is verified and validated. Results of the model verification are shown in Fig. 8 for one specific case (specimen #1). Similar studies are made for all the eight specimens. Based on the mesh sensitivity analysis, all the web subpanels should be divided at least into ten finite elements leading to appropriate resistance.

The model validation is executed at first 1) by the comparison of the numerical results to the test-based measured resistances and 2) by the comparison of the computed and measured failure modes. Results show that the developed numerical model is highly accurate. The calculated resistances are summarised in Tab. 1 for all test specimens and the comparison of the failure modes is presented for one case (specimen #2) in Fig. 9.

Results prove that the developed numerical model gives safe side resistances with the applied most detrimental imperfection configurations in case of all test specimens. Therefore, based on the verification and validation of the numerical model, the accuracy of the model is proved and considered to be appropriate for further numerical parametric study.

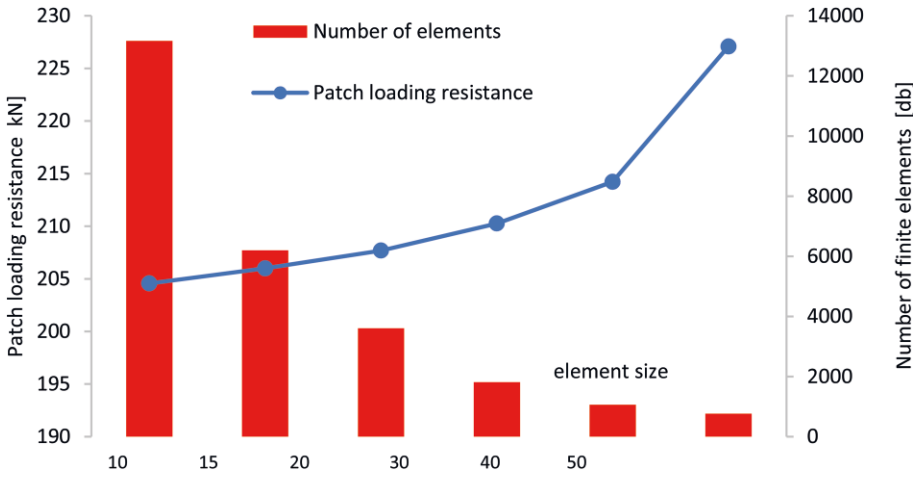

Fig. 8 Results of the model verification (specimen #1)

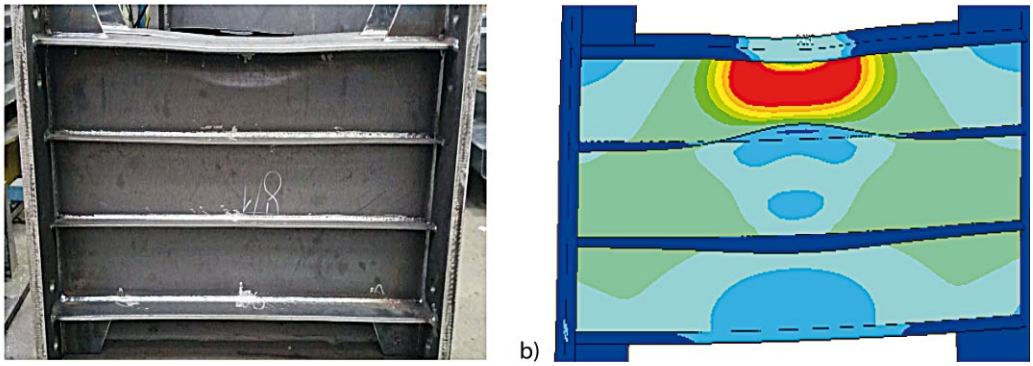

Fig. 9 Results of the model verification (specimen #2)

4.4 Results of the numerical parametric study

An extensive numerical parametric study is executed to analyse the patch loading failure mode and identify the trends of the different geometric parameters on the structural behaviour and resistance. The numerical parametric study have two separated parts but refer to the same geometrical configurations.

1. investigation of the critical load (F_{cr}) and
2. investigation of the patch loading resistance (F_{ult}).

A total of 2500 different girder geometries are investigated and for all geometrical configurations the buckling load (F_{cr}) and the patch loading resistance (F_{ult}) are determined. Within the parametric study, the parameters listed in Tab. 2 are varied within the given parameter ranges. All notations are given in Fig. 2. All the calculations are executed using S355 steel grade. The number of longitudinal stiffeners is varied between 2 and 4. The size of the stiffeners has been changed between a large extent to be able to investigate relatively weak and very strong stiffeners. The stiffener stiffness was the key parameter in the stiffener geometry selections. By changing the geometrical parameters, the following characteristic parameter ratio ranges are investigated: b_1/h_w = 0.15 to 0.45, h_w/t_w = 80 to 500, b_1/t_w = 25 to 167, and s_s/a = 0.2 to 0.8, whose parameter ranges refer to the typical geometries used for bridges.

Within the numerical parametric study, it was investigated first, how the stiffener stiffness (γ_s) does influence the patch loading resistance. Some of the obtained results are presented in Fig. 10 for girders having two longitudinal stiffeners varying the stiffener size between 40 × 4 mm and 80 × 10 mm. The size of the web for this specific case is 1100 × 6 mm, the flanges are made from steel plates with a size of 220 × 16 mm. All the numerical calculations show similar trends as presented in Fig. 10. If weak stiffeners are applied on the web, or no stiffeners are used, the failure mode is global buckling of the entire web panel. By increasing the stiffener stiffness, the patch loading resistance increases until the global buckling failure mode turns into local buckling, where further increase in the stiffener size does not affect the resistance, as shown in Fig. 10. The patch loading resistance values show a clear trend which has an increasing part and a quasi-constant domain. The intersection points between these two different structural behaviours can be determined and used as a characteristic measure for the separation of the global and local failure modes.

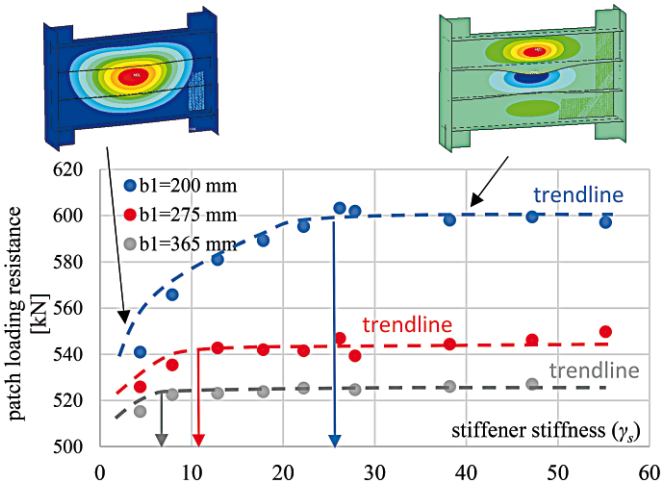

Fig. 10 Effect of stiffener stiffness on patch loading resistance

Tab. 2 Varied parameters and studied parameter ranges

	a [mm]	h_w [mm]	t_w [mm]	b_f [mm]	t_f [mm]	s_s [mm]
Min.	2400	1200	3	260	12	200
Max.	6000	4000	20	600	40	2000
	b_1 [mm]	h_{st} [mm]	t_{st} [mm]	γ_s	b_1/h_w	b_1/t_w
Min.	250	80	4	60	0.15	25
Max.	1000	290	20	4600	0.45	167

Within the numerical parametric study, the minimum stiffener stiffness is determined for all analysed girder geometries, which can ensure local buckling-type failure mode within the subpanel of the web. The calculation results show, all these minimum stiffness values were smaller (sometimes significantly smaller) than the maximum stiffener stiffness given by Eq. (10) to be allowed to consider in the critical buckling load according to EN 1993-1-5 [1].

It is also found this limit value returns usually smaller stiffener stiffness values, which are used in the bridge design praxis. It means that the main part of the real practical cases is designed using so-called 'strong' stiffeners, which are able to localise the buckling failure within the subpanel. Therefore, in further studies, only girders having 'strong' stiffeners are investigated and the obtained results and tendencies are valid for the local buckling-type failure mode where strong stiffeners ensure the separation of the buckling shapes within the web subpanels.

$$\gamma \left(\frac{\alpha}{h_w}\right)^3 \left(0.3 - \frac{b_1}{\alpha}\right)_{s.\lim} \tag{10}$$

$$\text{where } \gamma_s = 10.9 \cdot \frac{l_{s,l}}{h_w \cdot t_w^{\,3}} \tag{11}$$

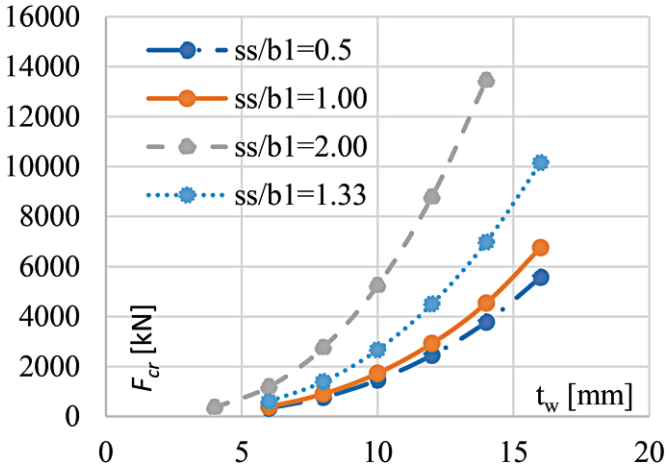

Fig. 11 Effect of stiffener stiffness on the critical buckling load

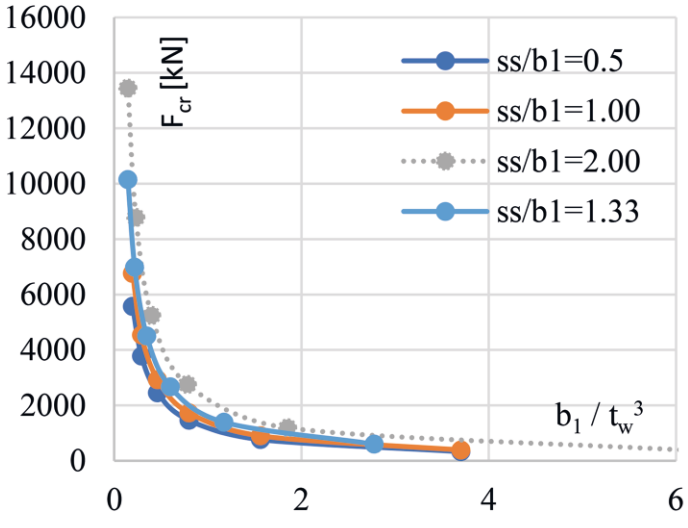

Fig. 12 Effect of stiffener stiffness on the critical buckling load

The effects of the main geometrical parameters on the critical buckling load are determined separately and evaluated on graphs. The main parameters have an influence on the critical buckling load and their trends are shown in Figs. 11 to 12. The horizontal axis of each graph shows the analysed geometrical parameter and the vertical axis shows the value of the critical buckling load.

Results prove that the critical buckling load increases by increasing the thickness of the web (t_w), the load introduction length (s_s), and by decreasing the subpanel depth (b_1). There is a clear trend shown in Fig. 12 between b_1/t_w^3 ratio and the critical buckling load. The same trend can be obtained for various s_s/b_1 ratios, making the entire evaluation process dimensionless. Further studies show there are other parameters which might slightly influence the patch loading resistance and the critical buckling load. For example, increase in the flange size (b_f, t_f) can cause increase in the critical buckling load; however, this effect is marginal compared to the previously presented parameters. The trend for each parameter is determined that only one parameter was changed within the study to be able to clearly separate the effect of each parameter independently.

5 The developed enhanced analytical resistance model

Based on the results of the numerical parametric study, the calculation method of the critical buckling load and the reduction factor for the ultimate load calculation are evaluated, and enhanced design equations are proposed for both. The numerical results prove that the critical buckling load should be calculated for the analysed failure mode based on the b_1/t_w^3 ratio instead of the h_w/t_w^3 ratio; therefore, the original design equation of the EN 1993-1-5 [11] has been changed to Eq. (12). Within this equation, all the other terms are kept unchanged and only this ratio is modified.

$$F_{cr} = 0.9 \cdot k_F \cdot E \cdot \frac{t_w^{\,3}}{b_1} \tag{12}$$

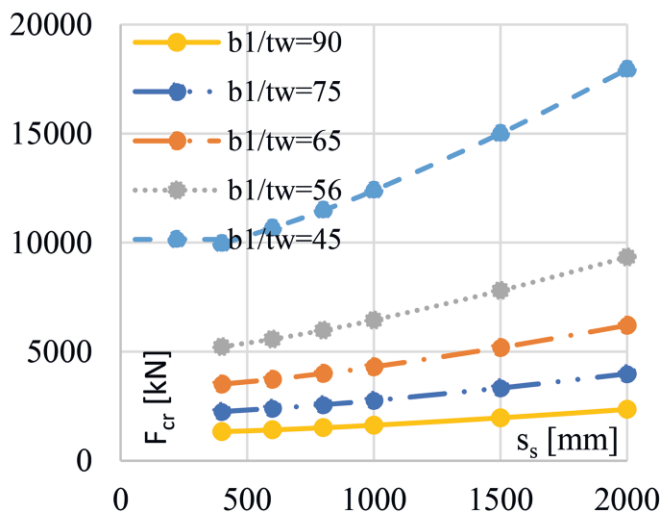

From the numerically calculated buckling load using Eq. (12) the required values of the k_F buckling coefficient are back calculated. It is proved that the mostly dominant parameter within the buckling coefficient is the s_s/b_1 ratio, whose trend is shown in Fig. 13 for geometries using closed section longitudinal stiffeners. Further evaluation proved that the buckling coefficient slightly depends on the b_1/t_w and $((b_f \cdot t_f^3)/(b_1 \cdot t_w^3))$ ratios as well. The most accurate equation for buckling coefficient is given by Eq. (13), in which the first two terms govern the calculation. The red line shown in Fig. 13 presents the

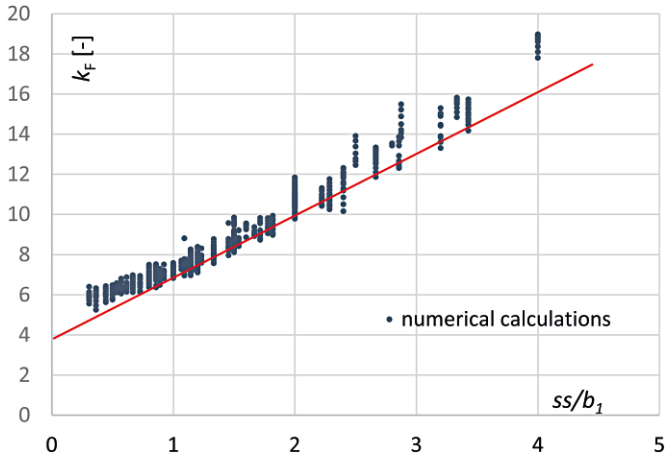

Fig. 13 Effect of s_s/b_1 ratio on the buckling coefficient

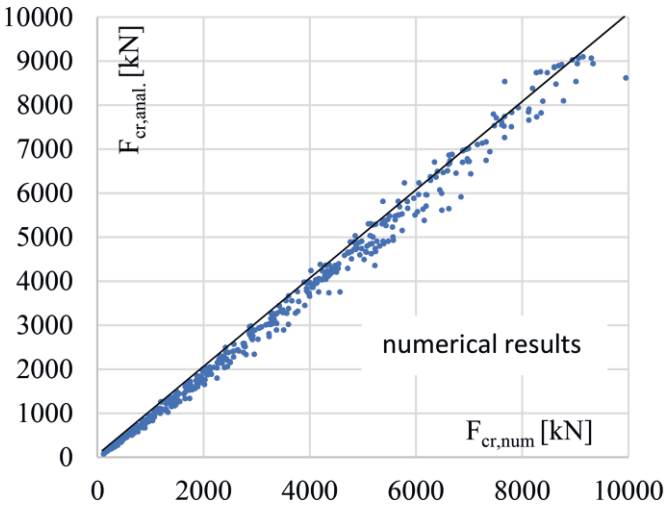

Fig. 14 A comparison of numerically and analytically calculated buckling load

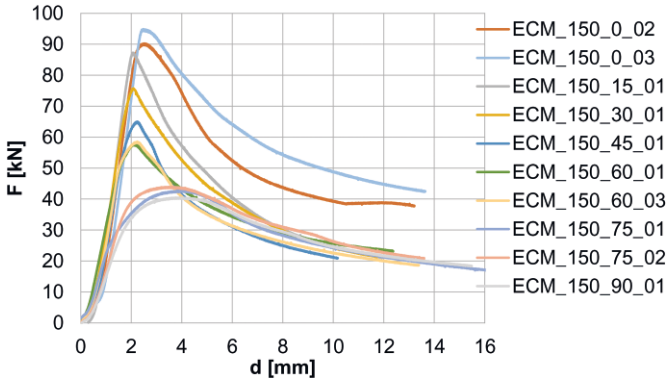

Fig. 15 Back-calculated reduction factors for the patch loading resistance

design equation containing only the first two terms, where the results only depend on the b_1/t_w ratio.

$$k_F = 4.0 + 3.0 \cdot \frac{s_s}{b_1} - 0.01 \cdot \frac{b_1}{t_w} + 0.2 \cdot \sqrt[4]{\frac{b_f \cdot t_f^3}{b_1 \cdot t_w^3}} \quad (13)$$

A comparison of the analytically and numerically calculated buckling loads is given in Fig. 14, where the analytical solution uses Eqs. (12) to (13) for the critical load and buckling coefficient calculation, respectively. For the entire database, the average and the maximum difference is 4.3 % and 17.3 %, respectively, with a standard deviation equal to 0,05.

The numerical calculations prove that the closed section stiffeners coming from its torsional rigidity provide larger buckling coefficients for the web. A similar numerical study as presented earlier is also executed for girders having open section flat plate longitudinal stiffeners. The results show that the same geometric parameters have an influence on the patch loading resistance and critical buckling load values; however, the buckling coefficient is smaller, coming from the smaller torsional rigidity, and its accurate value might be calculated by Eq. (14). This equation is similar to the first two terms of Eq. (13), by just changing the constant from 3.0 to 1.5.

$$k_F = 4.0 + 1.5 \cdot \frac{s_s}{b_1} \quad (14)$$

A comparison of the analytical results to the numerically computed values shows the average difference of 1.9 % with a standard deviation equal to 0.1.

Using the improved buckling load, the relative slenderness of all the analysed girders is calculated and the necessary reduction factors are back calculated from Eq. (1) using the effective loaded length determined by Eq. (6). Results are presented in Fig. 15. The horizontal axis shows the relative slenderness ratio according to Eq. (4) using the analytically calculated critical load (F_{cr}). The vertical axis shows the back-calculated reduction factors (χ_F).

Results prove the analytical solution using the improved buckling load and the currently proposed effective loaded length calculation method, and the buckling curve related to patch loading resistance gives safe side resistances. The red dashed line presenting the design value of the reduction factor (with partial safety factor equal to γ_{M1} = 1.1) gives a lower-bound curve for all the 2500 numerical simulation results. It proves that the current design method of the EN 1993-1-5 would give safe side resistances using the improved and more accurate buckling loads as well. However, results also show that there is a large scatter in the obtained resistance values and therefore, a more appropriate calculation method could be developed. Considering Eqs. (15) to (16), it can be observed that the relative slenderness and also the back-calculated reduction factor also depend on the effective loaded

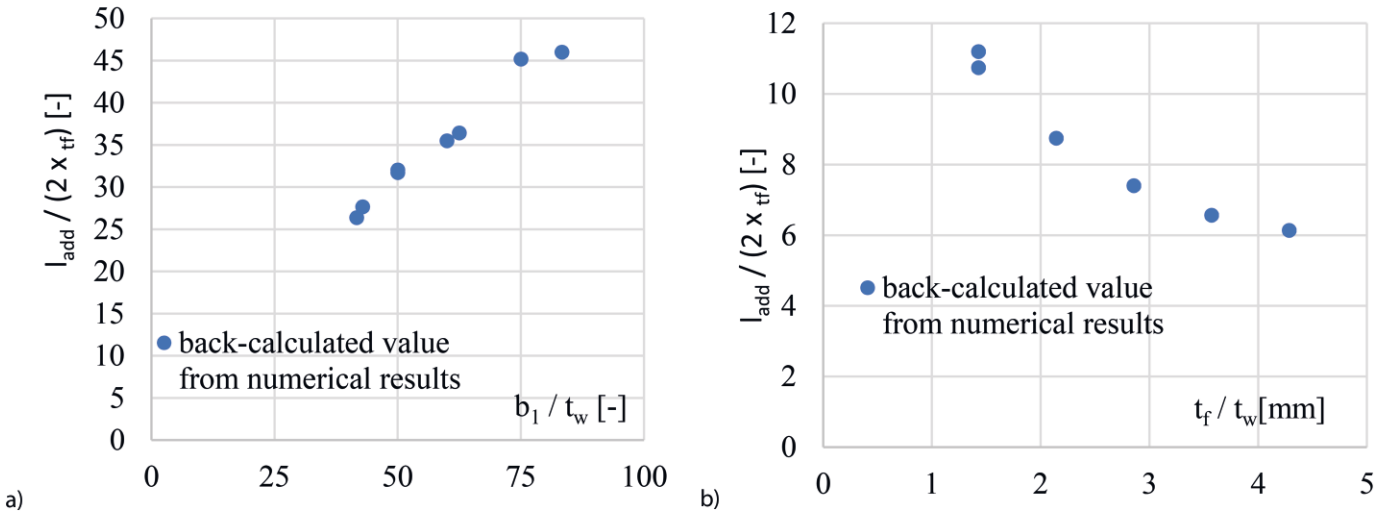

Fig. 16 Back-calculated effective loaded length depending on the a) b_1/t_w ratio and b) t_f/t_w ratio

length (l_y). All the other parameters of the calculation process are geometrical (t_w) or material (f_y) constants.

$$\bar{\lambda}_F = \sqrt{\frac{l_y \cdot t_w \cdot f_{yw}}{F_{cr}}} \tag{15}$$

$$F_{Rd} = \chi_F \cdot \frac{l_y \cdot f_{yw} \cdot t_w}{\gamma_{M1}} \leq 1.0 \tag{16}$$

Therefore, the accurate values for the effective loaded length are back calculated from the numerical calculation results and the main dominant parameters, which have influence on it, are determined. The value of the effective loaded length has two terms. At first, the loading length (s_s), which has a physical meaning, and its value can be considered as a given constant parameter for all analysed cases. Therefore, its effect has been separated and the equation of l_y is modified according to Eq. (17). The accurate value of the second term (l_{add}) is determined to each analysed geometry and evaluated in a detailed manner. The second term of Eq. (17) should have a physical meaning and its value should depend on the analysed girder geometry, especially on the size of the loaded flange and the web subpanel b_i/t_w ratio.

$$l_y = s_s + 2 \cdot t_f \cdot \left(1 + \sqrt{\frac{b_f}{t_w}}\right) = s_s + l_{add} \tag{17}$$

Results show that the main parameters which have influence on the effective loaded length are the loading length (s_s) and the b_1/t_w and t_f/t_w ratios. The determined trends are shown in Fig. 16.

The diagram shows that the effective loaded length increases, if the b_1/t_w ratio increases. The value decreases, if the t_f/t_w ratio increases. The physical meaning of these results is that if the web plate is weaker compared to the flange, the flange can better distribute the concentrated force along the web, and the patch load can result in a more uniform stress distribution, which can lead to larger effective loaded length.

Based on the numerical results, an improved equation is developed for the more accurate determination of the effective loaded length given by Eq. (18).

$$l_y = \begin{cases} s_s + 2 \cdot t_f \cdot \left[\sqrt{\frac{t_w}{t_f}} \cdot \left(0.5 \cdot \frac{b_1}{t_w} - 10\right)\right] \\ \text{if } 20 < \frac{b_1}{t_w} \leq 70 \\ s_s + 2 \cdot t_f \cdot \left[\sqrt{\frac{t_w}{t_f}} \cdot 0.2 \cdot \frac{b_1}{t_w} \cdot \frac{b_1}{s_s}\right] \\ \text{if } \frac{b_1}{t_w} > 70 \end{cases} \tag{18}$$

The effective loaded length has also a physical meaning. In addition, it adjusts the value of the numerically calculated datapoints presented in Fig. 17 not only along the vertical but also along the horizontal axis. It means that by an accurate determination of the effective loaded length, the scatter obtained in the numerical simulation results can be significantly reduced. Fig. 17 shows the back-calculated reduction factors using the improved equation for the effective loaded length.

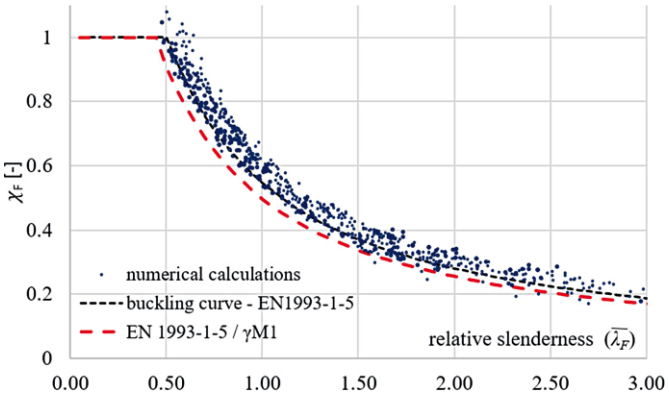

Fig. 17 Back-calculated reduction factors for the patch loading resistance using improved buckling load and effective loaded length

Results prove that the scatter has been significantly reduced and almost all the calculation results are on the safe side using the patch loading-type buckling curve of EN 1993-1-5 [11] with partial safety factor equal to $\gamma_{M1} = 1.1$. The average ratio of the analytical and numerical results has been changed to 0.91 with a standard deviation of 0.07, whose values prove the accuracy of the new improved design equation to determine the patch loading resistance of girders with multiple longitudinal stiffeners. If the results without considering $\gamma_{M1} = 1.1$ is executed, the average ratio would be 0.97 with a standard deviation of 0.06. A comparison of the numerically and analytically calculated patch loading resistances is also presented in Fig. 18.

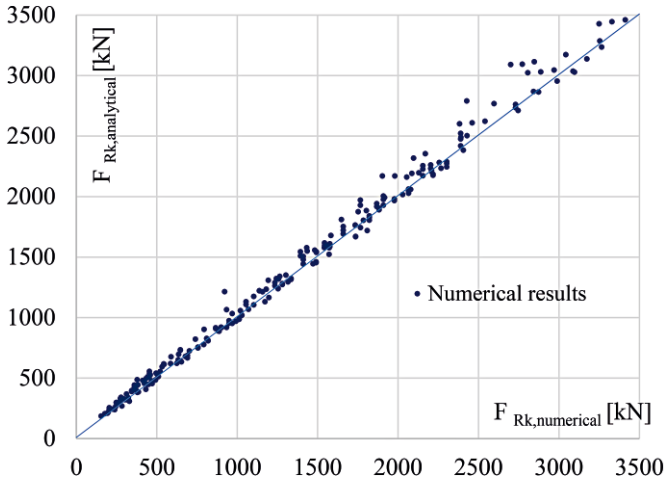

Fig. 18 A comparison of numerically and analytically calculated patch loading resistances

6 Effect of nonuniformly placed longitudinal stiffeners

The developed resistance model introduced in Section 5 is developed for the special case if the longitudinal stiffeners are uniformly placed along the web depth. However, in the case of real structures, the distance between the longitudinal stiffeners is usually not perfectly equal and there might be small differences in the subpanel depths (noted by b_1 and b_2, as shown in Fig. 19). The effect of the difference between the b_1 and b_2 values is investigated and presented in this section.

A numerical parametric study is executed by changing the b_1/b_2 ratio of the analysed girders, and the patch loading resistances are determined. Within the parametric study, the same parameter range is investigated as introduced in Section 4 with steel grade of S355. An example for three different girder geometries having different web thick-

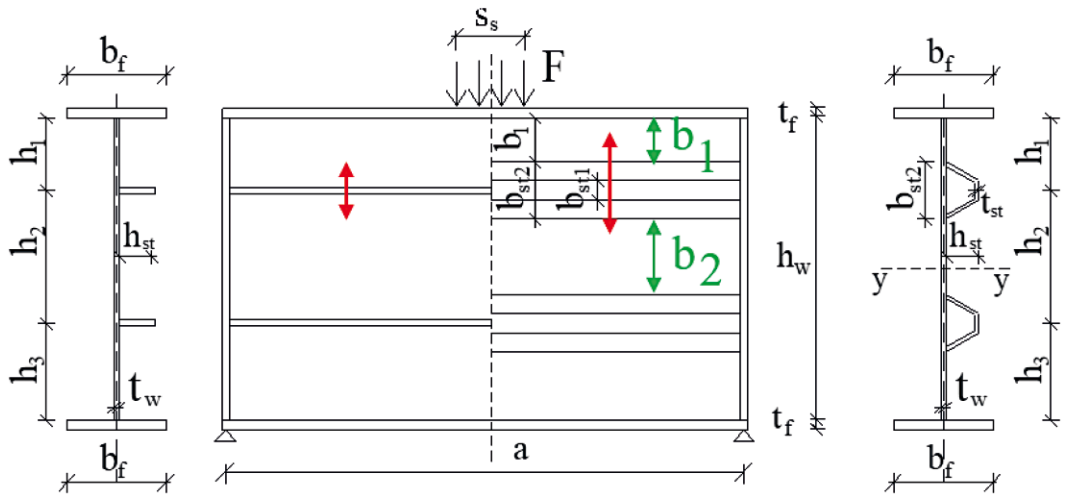

Fig. 19 Notations of b_1 and b_2 changed in the numerical parametric study

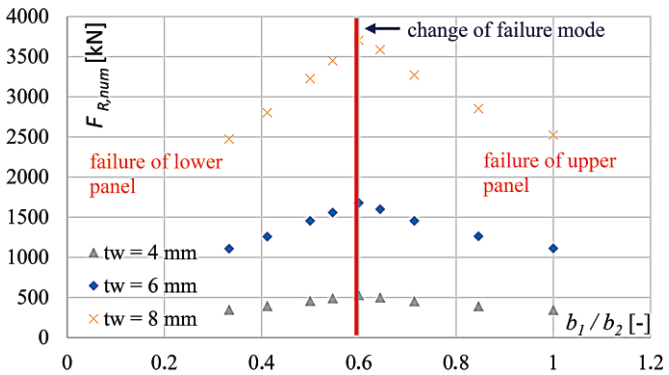

Fig. 20 Effect of the b_1/b_2 ratio and web thickness on the patch loading resistance and failure modes.

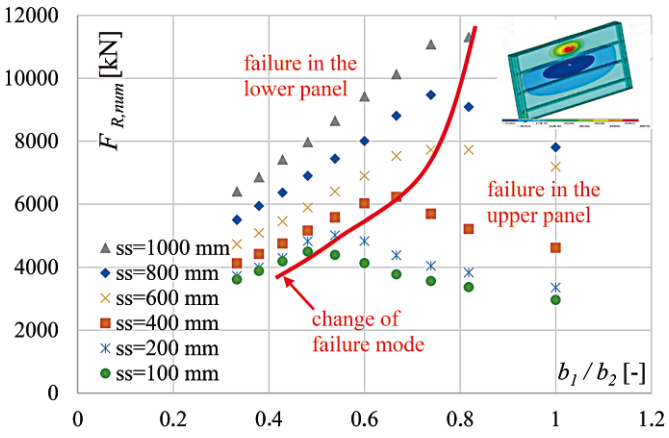

Fig. 21 Effect of the b_1/b_2 ratio and loading length on the patch loading resistance and failure modes

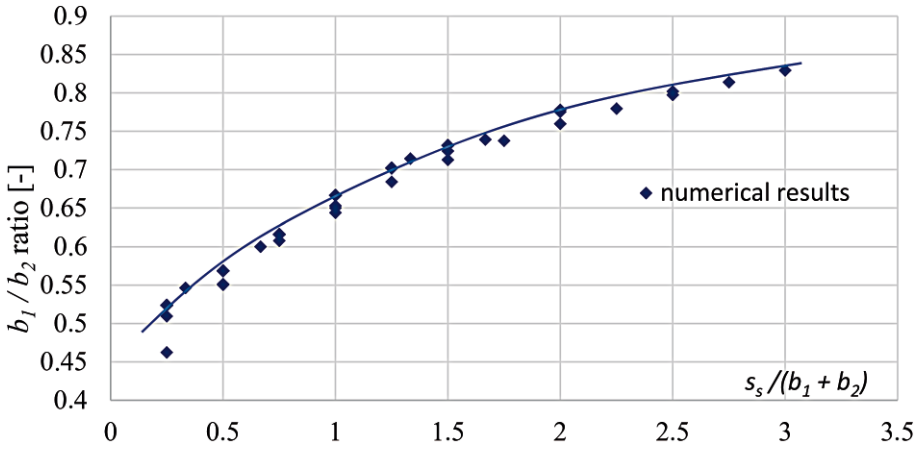

Fig. 22 Critical b_1/b_2 ratios leading to the failure mode change depending on the $s_s/(b_1+b_2)$ parameter

nesses is shown in Fig. 20. The results prove that if the b_1/b_2 ratio is small, the failure comes in the second (lower) subpanel of the girder. If the b_1/b_2 ratio is increased, the patch loading resistance increases until a maximum (optimum) value is reached. For higher values of the b_1/b_2 ratio, the failure comes in the upper subpanel and the patch loading resistance decreases by reaching the minimum value at $b_1/b_2 = 1.0$. If the subpanel depths are equal ($b_1 = b_2$), the failure always comes in the upper subpanel. The maximum points of the diagram always represent the change in the failure mode, shown by a red line in Fig. 20. A similar comparison is shown in Fig. 21 for girder geometries loaded by different loading lengths. It can be observed that the failure mode change does not depend on the web thickness (does not depend on the web panel slenderness), but it significantly depends on the loading length, as shown in Fig. 21.

Based on the large number of numerical simulation results, it has been observed that the b_1/b_2 ratio leading to the maximum patch loading resistance (whose value characterises the failure mode change) can be described by the ratio of the $s_s/(b_1+b_2)$ parameter, as shown in Fig. 22. In the current parametric study, the b_1+b_2 value was kept always constant by modifying the b_1/b_2 ratio.

These results mean that if the actual b_1/b_2 ratio of the analysed girder is larger than the values shown in Fig. 22, the failure will always occur in the upper subpanel and the patch loading resistance model introduced in Section 5 leads to safe side resistance. In another words, if the b_1/b_2 ratio is larger the limit value defined by Eq. (19), the newly developed patch loading resistance model can be safely applied, even if longitudinal stiffeners are not placed in equal distances.

$$\frac{b_1}{b_2} \geq \left(\frac{ss}{b_1+b_2}\right)^{0.15} - 0.35 \tag{19}$$

7 M–F interaction resistance

One more important point for the applicability of the newly developed patch loading resistance model is its applicability within interaction equations. In case of bridge launching, a large accompanying bending moment always acts together with the transverse force; therefore, the check of M–F interaction is a crucial task of the design process. A numerical parametric study has been executed to check the applicability of the newly developed patch loading resistance model in M–F interaction equations. According to the rules of EN 1993-1-5:2006 [1], if the girder is subjected to a concentrated transverse force acting on the compression flange in conjunction with bending and axial force, the resistance should be verified using the following interaction expression.

$$\eta_2 + 0.8 \cdot \eta_1 \leq 1.4 \tag{20}$$

where

η_1: utilisation ratio against normal stresses coming from normal force and bending moment and

η_2: utilisation ratio against transverse force.

Braun and Kuhlmann executed one of the latest researches on the M–F interaction behaviour of slender welded plated structures. The aim of their investigation was to collect all the previous experimental and numerical results and to re-evaluate all the previously developed M–F interaction equations compared to the experimental and numerical results. Finally, a new interaction equation given in form of Eq. (21) was proposed by Braun [19] in his Ph.D. thesis.

$$\left(\frac{F}{F_R}\right) + \left(\frac{M}{M_{pl,R}}\right)^{3.6} \leq 1.0 \tag{21}$$

where

$M_{pl,R}$: is the design plastic resistance of the cross section consisting of the effective area of the flanges and the fully effective web irrespective of its cross-section class and

F_R: patch loading resistance of the loaded web panel.

Based on their previous investigations on the M–F and V–F interaction fields and based on the results of the previous numerical calculations, Braun and Kuhlmann developed a combined interaction equation for the M–V–F interaction behaviour in the form of Eq. (22).

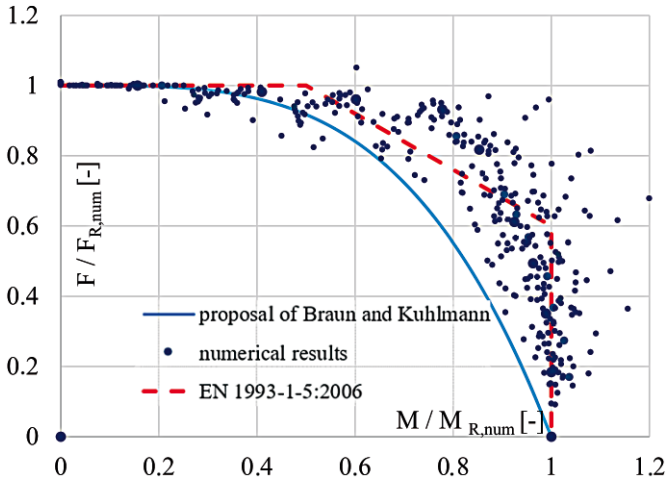

Fig. 23 M–F interaction resistances using the numerically calculated bending and patch loading resistances ($F_{R,num}$; $M_{R,num}$)

$$\left(\frac{M}{M_{pl,R}}\right)^{3.6}+\left(\frac{V-0.5\cdot F}{V_R}\right)^{1.6}+\left(\frac{F}{F_R}\right)\le 1.0 \qquad (22)$$

V, F, and M: shear force, transverse force, and bending moment acting on the loaded panel,

V_R: shear buckling resistance of the loaded web panel,

F_R: patch loading resistance of the loaded web panel, and

$M_{pl,R}$: is the design plastic resistance of the cross section consisting of the effective area of the flanges and the fully effective web irrespective of its cross-section class.

Eq. (21) represents the M–F plane of this 3D interaction equation, which will be used in this paper comparing to the numerical results. An additional numerical parametric study has been executed to study the bending moment and patch loading interaction behaviour of multiple stiffened girders. The same evaluation methodology and research strategy is used, which was previously described and introduced by Kövesdi et al. in [20, 21]. At first, the pure bending moment resistance of the analysed girders is determined 1) by hand calculations using the analytical design equations and 2) by the numerical model. Then the patch loading resistance has been determined (by small accompanying bending moment, which cannot be totally eliminated by applying transverse forces) by the numerical model and also by the newly developed resistance model introduced in Section 5. Then, for each analysed cross-section geometries, ten different bending moments and transverse force combinations (M–F interaction pairs) are analysed and the resistances are determined by the numerical model.

The results of the numerical parametric study are presented in Fig. 23 using the numerically calculated bending ($M_{R,num}$) and patch loading resistances ($F_{R,num}$) as reference values. It can be seen that several datapoints representing a large transverse force and small bending moment are inside the interaction curve, which means that the interaction resistances of the girders are slightly smaller than those predicted by the M–F interaction curve. In the range of large bending moments and small transverse forces, there are no datapoints on the unsafe side. The reason for it is that the M–F interaction curve proposed by Braun and Kuhlmann is applicable together with analytical-based patch loading and bending resistance models.

Therefore, the same evaluation process is executed using the analytically calculated patch loading and bending resistances. Thus, the plastic bending resistance is used in Eq. (21). The evaluation of the numerical results is done at first using the numerically calculated bending resistance considering the actual cross-section class and then using the plastic moment resistance irrespective of the cross-section classes. Results for both are presented in Fig. 24. The vertical axis of these diagrams shows for both

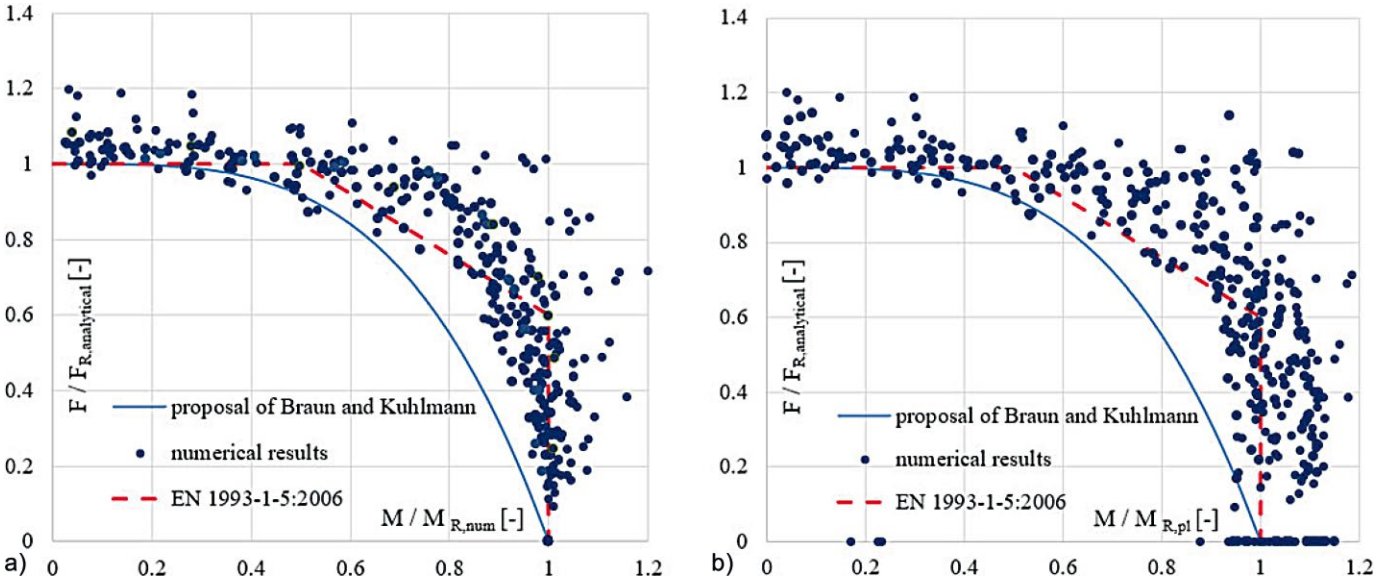

Fig. 24 M–F interaction resistances using the a) numerically calculated bending and analytically calculated patch loading resistances ($F_{R,analytical}$; $M_{R,num}$) and b) analytically calculated plastic bending and patch loading resistances ($F_{R,analytical}$; $M_{R,pl}$).

cases the patch loading resistance divided by the analytically calculated patch loading resistance according to Section 5.

The horizontal axis shows the bending moment resistances divided by the numerically calculated and plastic moment resistance, respectively. Results prove that the M–F interaction equation according to Eq. (21) leads to safe side resistances using both the numerically calculated moment resistance and the plastic moment resistance. It proves the applicability of the new patch loading resistance model in the M–F interaction equation.

8 Conclusions

The present article introduces an improved design method for the patch loading resistance of multiple stiffened girders. An extensive research programme is conducted to determine the accurate value of the patch loading resistance. The executed research consists of laboratory experiments, extensive numerical investigations, and development of analytical design equations. The new findings based on the research results are the following.

- It has been shown that the failure modes can be separated between local and global buckling based on the stiffness criterion of the longitudinal stiffeners.
- Minimum stiffness criterion is determined to identify the local buckling failure within the loaded subpanel of the web.
- Design equation is developed for the critical buckling load calculation for the local buckling-type failure mode.
- Improved design equation is developed for the novel calculation of the effective loaded length.
- It has been proved that using the improved design equations for the critical buckling load and the effective loaded length, the buckling curve of EN 1993-1-5 can be used with adequate safety to determine the patch loading resistance.
- Geometrical limit values for the application range of the new resistance model are derived ensuring buckling failure within the upper subpanel.
- Applicability of the new patch loading resistance model with the previously developed M–F interaction equation is proved.

Acknowledgements

The presented research programme was financially supported by the Grant MTA-BME Lendület LP2021-06/2021 ‘theory of new generation steel bridges’ programme of the Hungarian Academy of Sciences, which is gratefully acknowledged.

References

[1] EN 1993-1-5:2005 (2006) *Eurocode 3: Design of steel structures. Part 1-5: Plated structural elements*. European Committee for Standardization.
[2] Lagerqvist, O. (1995) *Patch loading resistance of steel girders subjected to concentrated forces* [doctoral thesis, 1994:159D]. Luleå University of Technology, Division of Steel Structures, Luleå, Sweden.
[3] Lagerqvist, O.; Johansson, B. (1996) *Resistance of I-girders to concentrated loads*. Journal of Constructional Steel Research 39, No. 2, pp. 87–119.
[4] Graciano, C. A. (2002) *Patch loading – Resistance of longitudinally stiffened steel girder webs* [PhD doctoral thesis, 2002:18]. Luleå University of Technology, Division of Steel Structures, Luleå, Sweden.
[5] Graciano, C.; Johansson, B. (2003) *Resistance of longitudinally stiffened I-girders subjected to concentrated loads*. Journal of Constructional Steel Research 59, No. 5, pp. 561–586.
[6] Graciano, C. (2005) *Strength of longitudinally stiffened webs subjected to concentrated loading*. Journal of Structural Engineering ASCE 131, No. 2, pp. 268–278.
[7] Davaine, L. (2005) *Formulation de la résistance au lancement d’une âme métallique de pontraidie longitudinalement* [doctoral thesis, D05–05]. INSA de Rennes, France (in French).
[8] Gozzi, J. (2007) *Patch loading resistance of plated girders* [doctoral thesis, 2007:30]. Luleå University of Technology, Sweden. ISRN: LTU-DT-07/30–SE.
[9] Chacón, R.; Mirambell, E.; Real, E. (2010) *Hybrid steel plate girders subjected to patch loading, Part 2: Design proposal*. Journal of Constructional Steel Research 66, No. 5, pp. 709–715.
[10] Mirambell, E.; Chacón, R.; Kuhlmann, U.; Braun, B. (2021) *Statistical evaluation of the new resistance model for steel plate girders subjected to patch loading*. Steel Construction 1, No. 5, pp. 10–15. https://doi.org/10.1002/stco.201200003
[11] EN 1993-1-5:2024, *Eurocode 3: Design of steel structures. Part 1-5: Plated structural elements* (before publication). European Committee for Standardization.
[12] COMBRI (2007) *Competitive Steel and Composite Bridges by Improved Steel Plated Structures*. Final Report, RFCS Research Project RFS-CR-03018.
[13] Seitz, M. (2005) *Tragverhalten längsversteifter Blechträger unter quergerichteter Krafteinleitung* [doctoral thesis]. Universität Stuttgart, Mitteilung des Instituts für Konstruktion und Entwurf Nr.2005–2 (in German).
[14] Graciano, C.; Lagerqvist, O. (2003) *Critical buckling of longitudinally stiffened webs subjected to compressive edge loads*. Journal of Constructional Steel Research 59, No. 9, pp. 1119–1146.
[15] Graciano, C.; Mendes, J. (2014) *Elastic buckling of longitudinally stiffened patch loaded plate girders using factorial design*. Journal of Constructional Steel Research 100, pp. 229–236.
[16] Graciano, C. (2015) *Patch loading resistance of longitudinally stiffened girders – A systematic review*. Thin-Walled Structures 95, pp. 1–6.
[17] Kövesdi, B.; Mecséri, B.J.; Dunai, L. (2018) *Imperfection analysis on the patch loading resistance of girders with open section longitudinal stiffeners*. Thin-Walled Structures 123, pp. 195–205.
[18] Ansys, Inc. (2015) *ANSYS® v16.5* [software]. Canonsburg, Pennsylvania, USA.

[19] Braun, B. (2010) *Stability of steel plates under combined loading* [doctoral thesis, No. 2010-3]. Institute for Structural Design, Universität Stuttgart.

[20] Kövesdi, B.; Alcaine, J.; Dunai, L.; Mirambell, E.; Braun, B.; Kuhlmann U. (2014) *Interaction behaviour of steel I-girders under bending, shear and transverse force, part I: Longitudinally unstiffened girders*. Journal of Constructional Steel Research 103, pp. 327–343.

[21] Kövesdi, B.; Alcaine, J.; Dunai, L.; Mirambell, E.; Braun, B.; Kuhlmann U. (2014) *Interaction behaviour of steel I-girders under bending, shear and transverse force, Part II: Longitudinally stiffened girders*. Journal of Constructional Steel Research 103, pp. 344–353.

Authors

Dr. Balázs Kövesdi (corresponding author)
kovesdi.balazs@emk.bme.hu
Budapest University of Technology and Economics
Faculty of Civil Engineering, Department of Structural Engineering
Műegyetem rkp. 3.
1111 Budapest, Hungary

Prof. Dr. László Dunai
dunai.laszlo@emk.bme.hu
Budapest University of Technology and Economics
Faculty of Civil Engineering, Department of Structural Engineering
Műegyetem rkp. 3.
1111 Budapest, Hungary

How to Cite this Paper

Kövesdi, B.; Dunai, L. (2023) *Patch loading resistance of slender plate girders with multiple longitudinal stiffeners.* Steel Construction 16, No. 1, pp. 16–30. https://doi.org/10.1002/stco.202200047

This paper has been peer reviewed. Submitted: 1. December 2022; accepted: 9. January 2023.